

Preliminary Analysis of the Transient Reactor Test Facility (TREAT) with PROTEUS

Nuclear Engineering Division

About Argonne National Laboratory

Argonne is a U.S. Department of Energy laboratory managed by UChicago Argonne, LLC under contract DE-AC02-06CH11357. The Laboratory's main facility is outside Chicago, at 9700 South Cass Avenue, Argonne, Illinois 60439. For information about Argonne and its pioneering science and technology programs, see www.anl.gov.

DOCUMENT AVAILABILITY

Online Access: U.S. Department of Energy (DOE) reports produced after 1991 and a growing number of pre-1991 documents are available free via DOE's SciTech Connect (<http://www.osti.gov/scitech/>)

Reports not in digital format may be purchased by the public from the National Technical Information Service (NTIS):

U.S. Department of Commerce
National Technical Information Service
5301 Shawnee Rd Alexandria, VA 22312 www.ntis.gov
Phone: (800) 553-NTIS (6847) or (703) 605-6000
Fax: (703) 605-6900
Email: orders@ntis.gov

Reports not in digital format are available to DOE and DOE contractors from the Office of Scientific and Technical Information (OSTI):

U.S. Department of Energy
Office of Scientific and Technical Information
P.O. Box 62
Oak Ridge, TN 37831-0062
www.osti.gov
Phone: (865) 576-8401
Fax: (865) 576-5728

Disclaimer

This report was prepared as an account of work sponsored by an agency of the United States Government. Neither the United States Government nor any agency thereof, nor UChicago Argonne, LLC, nor any of their employees or officers, makes any warranty, express or implied, or assumes any legal liability or responsibility for the accuracy, completeness, or usefulness of any information, apparatus, product, or process disclosed, or represents that its use would not infringe privately owned rights. Reference herein to any specific commercial product, process, or service by trade name, trademark, manufacturer, or otherwise, does not necessarily constitute or imply its endorsement, recommendation, or favoring by the United States Government or any agency thereof. The views and opinions of document authors expressed herein do not necessarily state or reflect those of the United States Government or any agency thereof, Argonne National Laboratory, or UChicago Argonne, LLC.

Preliminary Analysis of the Transient Reactor Test Facility (TREAT) with PROTEUS

prepared by
H. M. Connaway and C. H. Lee
Nuclear Engineering Division, Argonne National Laboratory

November 30, 2015

EXECUTIVE ABSTRACT

The neutron transport code PROTEUS has been used to perform preliminary simulations of the Transient Reactor Test Facility (TREAT). TREAT is an experimental reactor designed for the testing of nuclear fuels and other materials under transient conditions. It operated from 1959 to 1994, when it was placed on non-operational standby. The restart of TREAT to support the U.S. Department of Energy's resumption of transient testing is currently underway.

Both single assembly and assembly-homogenized full core models have been evaluated. Simulations were performed using a historic set of WIMS-ANL-generated cross-sections as well as a new set of Serpent-generated cross-sections. To support this work, further analyses were also performed using additional codes in order to investigate particular aspects of TREAT modeling. DIF3D and the Monte-Carlo codes MCNP and Serpent were utilized in these studies. MCNP and Serpent were used to evaluate the effect of geometry homogenization on the simulation results and to support code-to-code comparisons. New meshes for the PROTEUS simulations were created using the CUBIT toolkit, with additional meshes generated via conversion of selected DIF3D models to support code-to-code verifications.

All current analyses have focused on code-to-code verifications, with additional verification and validation studies planned. The analysis of TREAT with PROTEUS-SN is an ongoing project. This report documents the studies that have been performed thus far, and highlights key challenges to address in future work.

TABLE OF CONTENTS

Executive Abstract	i
Table of Contents	ii
List of Figures	iii
List of Tables.....	i
1. Introduction.....	1
2. TREAT Description	2
2.1 Reactor Overview.....	2
2.2 Key Core Properties	5
3. TREAT Modeling and Simulation.....	7
3.1 MCNP Simulations	7
3.1.1 Homogenized Fuel Assembly in Infinite Lattice.....	7
3.1.2 Fuel Graphitization	10
3.1.3 Cross-section Library	11
3.2 PROTEUS-SN Simulations with Historic ISOTXS File	11
3.2.1 Homogenized Single Assembly Model	11
3.2.2 Full Core Model.....	12
3.3 Serpent Model Simulations.....	15
3.4 Multigroup Cross Section Generation.....	18
3.5 PROTEUS-SN Simulations with Serpent-generated Cross-sections.....	22
4. Conclusions.....	28
References	29

LIST OF FIGURES

Figure 1. Standard TREAT Fuel Assembly	3
Figure 2. Cross-section View of the TREAT Reactor	4
Figure 3. Illustration of the TREAT Hodoscope Configuration	4
Figure 4. Illustration of the Key Segments of a TREAT Control Rod	5
Figure 5. Lengthwise View of TREAT Fuel Assembly in MCNP, (a) Simplified Geometry and (b) True Geometry	8
Figure 6. Detailed MCNP Model of TREAT Fuel Assembly.....	9
Figure 7. Cross-sectional View of MCNP Model Similar to TREAT Minimum Critical Core	10
Figure 8. PROTEUS-SN Meshes Used for Infinite Lattice of Homogenized Assemblies, (a) 10x10x29 and (b) 20x20x29	12
Figure 9. PROTEUS-SN Model for TREAT, (a) Radial Slice and (b) Axial Slice.....	13
Figure 10. MCNP TREAT Core, (a) X-Y View and (b) X-Z View	14
Figure 11. Meshes Used in Current PROTEUS-SN Simulations – A, B, and C	14
Figure 12. Simplified Model of TREAT Fuel Assembly Used in MCNP and Serpent, (a) X-Y and (b) X-Z View	16
Figure 13. Geometries for Generating TREAT Fuel Assembly Cross Sections.....	19
Figure 14. ISOTXS Generation Using Serpent Multigroup Cross Section	20
Figure 15. Composition Assignment and Fast and Thermal Fluxes of the C5 Problem Resulting from Diffusion Calculation with the 23-group Multigroup Cross Sections from Serpent.....	21
Figure 16. 3D Fuel Assembly Problem (right) and Its Neutron Spectra (left) for TREAT	21
Figure 17. Example PROTEUS-SN Meshes for TREAT 2D Fuel Assembly Heterogeneous Fuel Region	23
Figure 18 Thermal Neutron Fluxes for PROTEUS-SN 2D Heterogeneous Fuel Region	23
Figure 19. Example 3D Heterogeneous TREAT Fuel Assembly Meshes for PROTEUS-SN	24
Figure 20. 3D PROTEUS Model of TREAT Minimum Critical Core Loading.....	25
Figure 21. Cross-section View of Example PROTEUS 3D Minimum Critical Core Mesh....	26
Figure 22. Cross-section View of Coarse PROTEUS Mesh for Control Rod Assembly	26
Figure 23. ν^*F Fission Rate Distribution at Fuel Section Mid-height in PROTEUS 3D Simulation of TREAT Minimum Critical Core with Control Rod Inserted	27

LIST OF TABLES

Table 1. Nine Energy Group Structure in WIMS-ANL-generated ISOTXS file.....	7
Table 2. MCNP Results for Infinite Lattice of Simplified TREAT Fuel Assemblies	8
Table 3. Axial Zones Featured in More Detailed MCNP Model of TREAT Fuel Assembly ...	9
Table 4. MCNP Homogenization Results for More Detailed TREAT Fuel Assembly Model	10
Table 5. TREAT MCNP Modeling with Different Cross-section Libraries	11
Table 6. Example Results for MCNP and PROTEUS-SN Simulations of Infinite Lattice of Homogenized, Simplified TREAT Fuel Assemblies	12
Table 7. DIF3D Results for Historic Minimum Critical Core Model with Void Boundary Conditions	13
Table 8. PROTEUS, MCNP, and DIF3D Results for Minimum Critical TREAT Core with Homogenized Assemblies and Reduced Radial Permanent Reflector.....	15
Table 9. MCNP and Serpent Simulation Results for Simplified TREAT Fuel Assembly	17
Table 10. Temperature Reactivity Feedback Estimate for MCNP and Serpent Simulations of Infinite and 19x19 Fuel Assembly Arrays	17
Table 11. Volume Fractions Used in Homogenization of TREAT Assembly.....	18
Table 12. 2D Serpent Simulation of TREAT Assembly Fuel Region	18
Table 13. 3D Serpent Simulation of Simplified TREAT Fuel Assembly.....	18
Table 14. MCNP Eigenvalues of TREAT Fuel Assembly with Different Geometries	19
Table 15. Eigenvalue Comparison for the C5 Benchmark Problem between MCNP, Serpent, and Diffusion (23-group MG cross sections).....	21
Table 16. Eigenvalues for 3D Full Core Problems (No Air Regions) with Different FA and CR Assembly Loadings	22
Table 17. PROTEUS-SN Results, 2D TREAT Assembly Heterogeneous Fuel Region	23
Table 18. 2D TREAT Fuel Region, Evaluation of PROTEUS-SN Simulation with Serpent- generated Homogenized Cross-sections	24
Table 19. Results for 3D Heterogeneous TREAT Assembly with Hypothetical Higher Density Material in the Gap.....	25

1. Introduction

The PROTEUS code is a high-fidelity three-dimensional deterministic neutron transport code developed at Argonne National Laboratory (ANL) as part of the Simulation-based High-efficiency Advanced Reactor Prototyping (SHARP) multiphysics toolkit under the U.S. Department of Energy (DOE) Office of Nuclear Energy's Nuclear Energy Advanced Modeling and Simulation (NEAMS) Program [1, 2]. Based on the second-order discrete ordinate transport method, PROTEUS-SN is a highly scalable code applicable to all neutron energy spectrum calculations. The code can accommodate unstructured finite element geometries, which allows for the modeling of complex or unconventional geometric reactor models.

In this study, PROTEUS-SN has been utilized to preform preliminary simulations of the Transient Reactor Test Facility (TREAT) located at the Idaho National Laboratory (INL). TREAT is an experimental reactor designed for the testing of nuclear fuels and other materials under transient conditions. It began operation in 1959, and was utilized for a wide variety of experiments until 1994, when it was placed on non-operational standby. Recently, the U.S. DOE has decided to pursue the resumption of transient testing in the United States using TREAT [3].

The restart of TREAT requires the renewed development of simulation models and methods to support the analysis of reactor operation and experiment planning. Highly detailed three-dimensional simulations of the core and experiment vehicle, which were not as feasible during TREAT operation given the limitations in computational resources at that time, now can be performed. Traditionally TREAT experiment planning required a number of preliminary calibration irradiations in order to evaluate the relationship between core and test sample behavior under both steady-state and transient conditions. It is expected that improved modeling and simulation will both provide better understanding of TREAT behavior and allow for more effective experimentation.

To support the work with PROTEUS-SN, additional simulations were also performed using other codes in order to investigate particular aspects of TREAT modeling. DIF3D and the Monte-Carlo codes MCNP and Serpent were utilized in these studies. New meshes for the PROTEUS-SN simulations were generated using the CUBIT toolkit, with additional studies also performed using meshes generated via the conversion of existing DIF3D models. Initial PROTEUS-SN simulations were performed using a historic cross-section set generated with the WIMS-ANL code. Simultaneously to this work, efforts were made to develop a method for generating new cross-sections using Serpent. Preliminary simulations with the new Serpent-generated cross-section set have also been performed. All current analyses have focused on code-to-code verifications.

2. TREAT Description

2.1 Reactor Overview

TREAT is a heterogeneous, air-cooled, graphite-moderated and graphite-reflected thermal reactor. A detailed description of TREAT can be found in the facility's 1960 design summary report [4]. The reactor is fueled with highly-enriched (~93%) UO₂ dispersed in graphite, with a fuel carbon-to-uranium (C/U) atomic ratio of roughly 10000 to 1. The fuel is arranged in zircaloy-clad fuel assemblies, with an approximately 4 ft long central fuel section and 2 ft long aluminum-clad graphite reflectors above and below the fuel. The assemblies are approximately 4 in x 4 in square, with chamfered corners. An illustration of a standard TREAT fuel assembly is provided in Figure 1. The reactor also utilized a variety of special-purpose assemblies, including:

- Control Rod Assemblies: assemblies with a 2 in diameter hole running axially through the center to accommodate a reactor control rod
- Dummy Assemblies: assemblies containing unfueled graphite in the place of UO₂ fuel
- Slotted Assemblies: assemblies with some (or all) of the fuel region removed in order to provide an unimpeded path for neutron travel to the hodoscope (described below)
- Thermocouple Assemblies: select set of standard assemblies with a limited number of thermocouples attached, which were placed in the locations anticipated to experience the hottest temperatures in a given experiment

The reactor core can accommodate a maximum of 361 assemblies, arranged in a 19x19 array. The core is surrounded by a permanent graphite reflector, which is in turn enclosed in a concrete bioshield. The reflector includes a set of movable blocks of graphite, which could be removed to provide viewing slots to the core. Both the reflector and bioshield have holes to accommodate instrumentation. The reactor layout is shown in Figure 2. The experiment vehicles for sample irradiation were placed at the center of the core, and typically replaced 1-4 fuel assemblies. Sample behavior during a transient was monitored by an ex-core system of collimated detectors called the hodoscope. Unfueled, air-filled slotted assemblies (described above) were typically used to provide an open path between the sample and hodoscope (Figure 3).

Reactor operation is controlled by a set of B₄C-bearing control rods. The rods consist of a poison section packed with boron carbide powder, with a zircaloy-clad graphite rod follower below this region, and additional stainless steel and graphite follower segments below that. An illustration of a TREAT control rod is provided in Figure 4. Transients are performed by introducing reactivity via the withdrawal (from a low power critical state) of a select set of control rods referred to as the Transient Bank. These transients are controlled by the large, prompt negative temperature reactivity feedback provided by the heating of the fuel graphite. The layout of the control rods within the core was changed in the late-1980s; core loadings prior to this change are referred to as the 'pre-upgrade core' and loadings following this change are referred to as the 'upgraded core'.

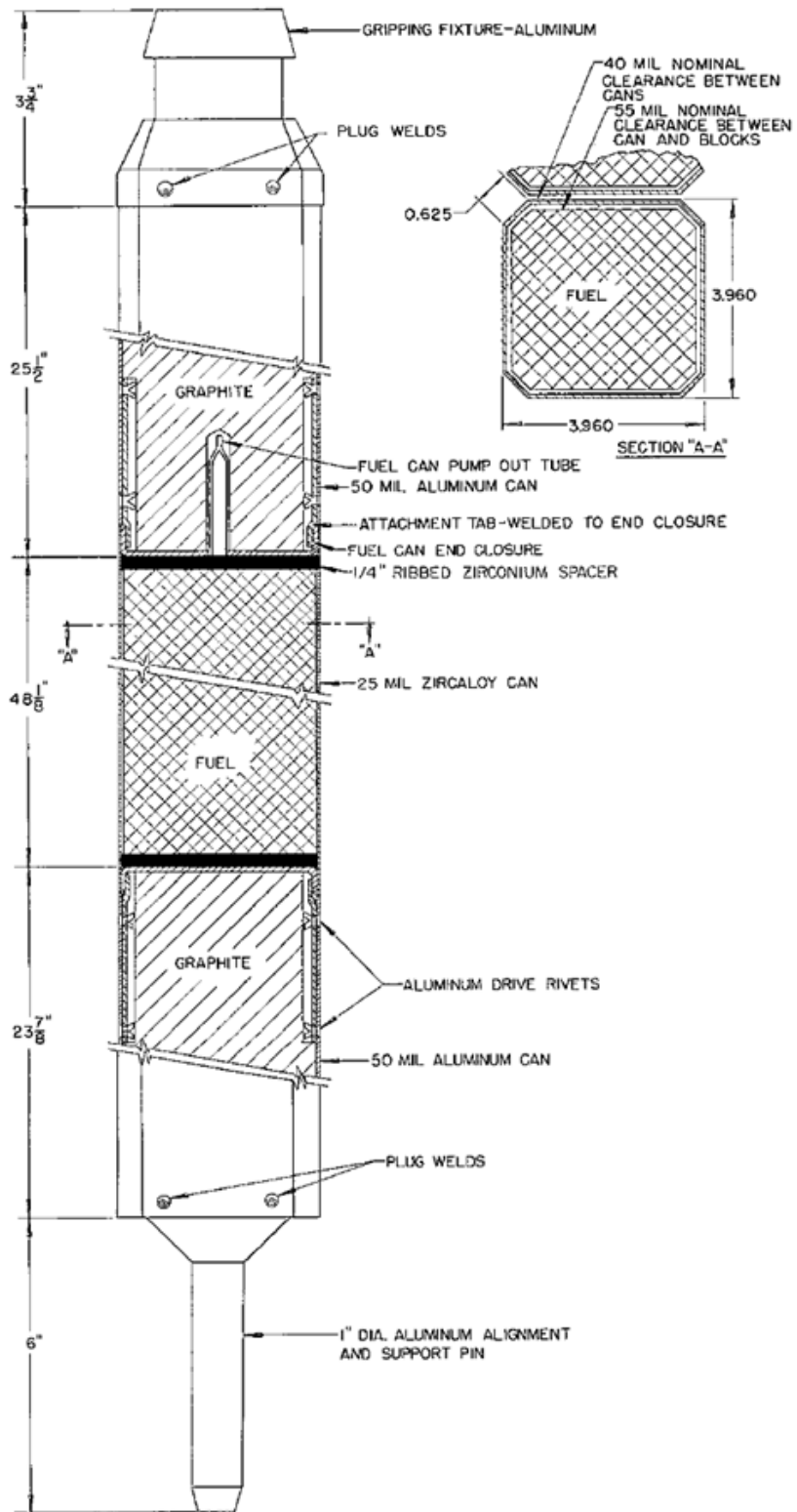


Figure 1. Standard TREAT Fuel Assembly

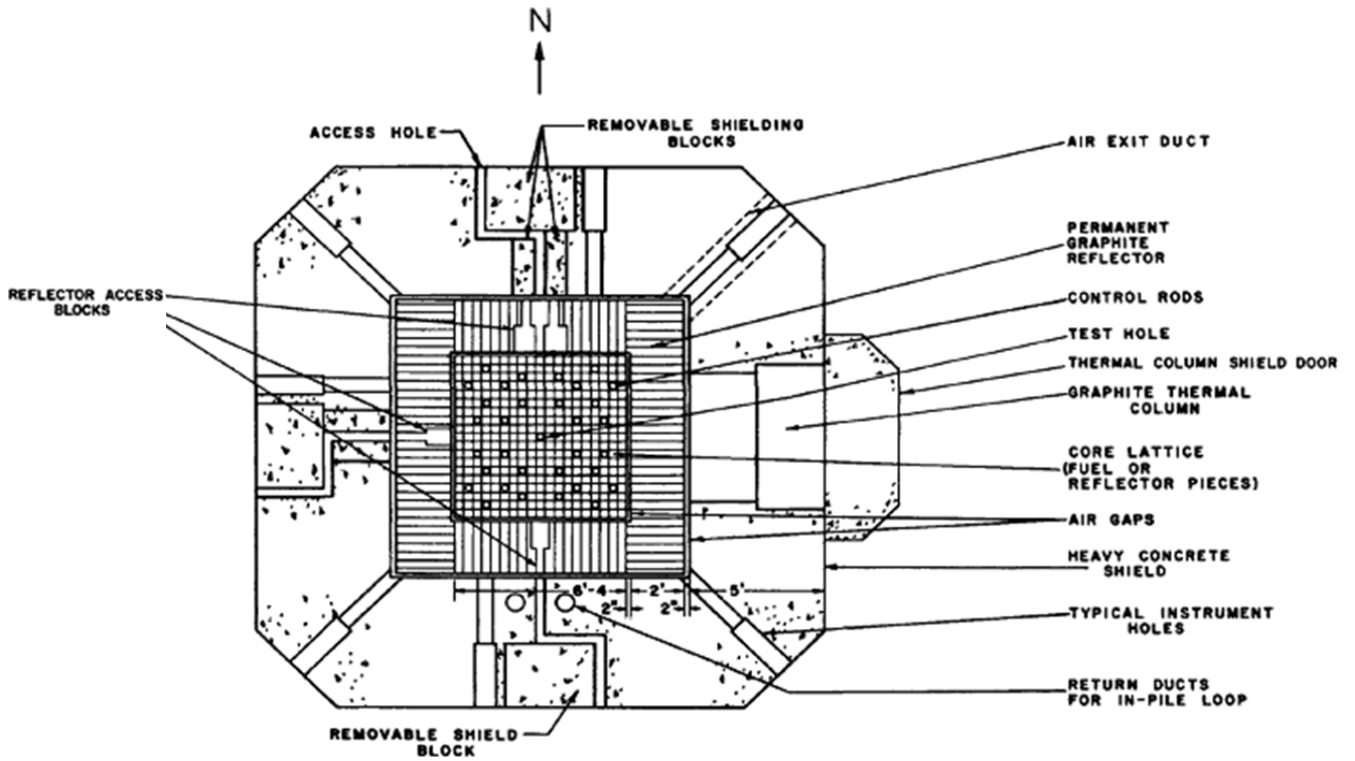


Figure 2. Cross-section View of the TREAT Reactor

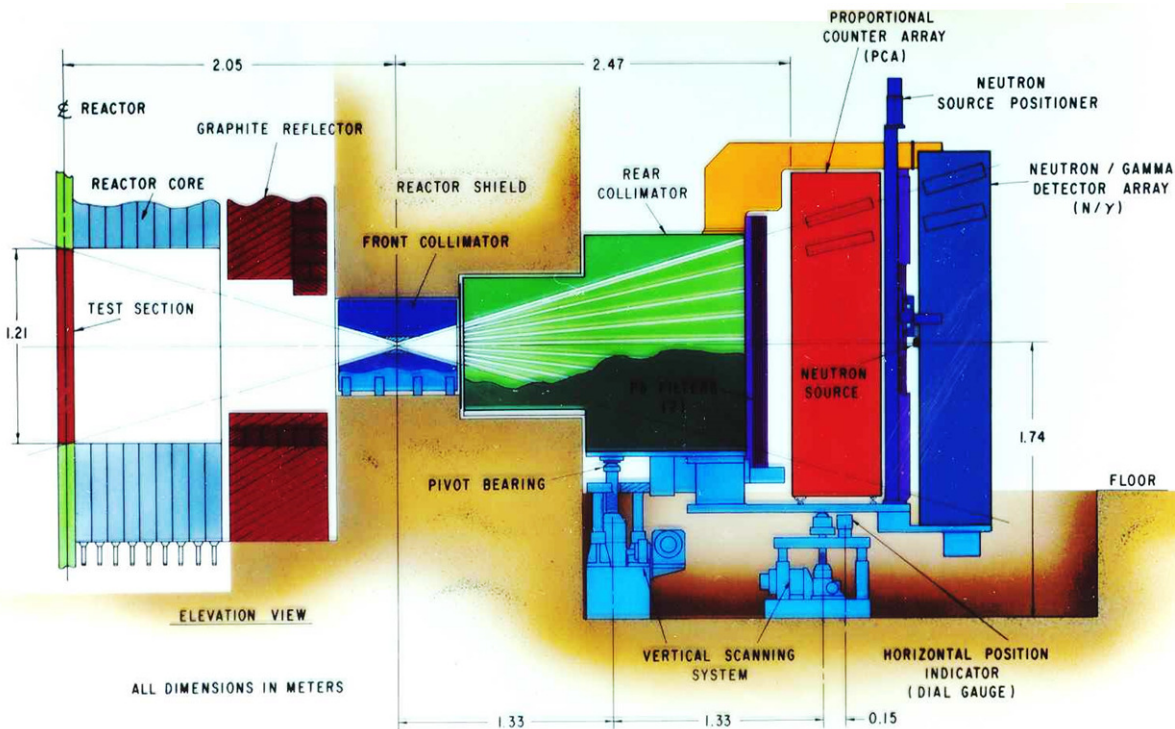


Figure 3. Illustration of the TREAT Hodoscope Configuration

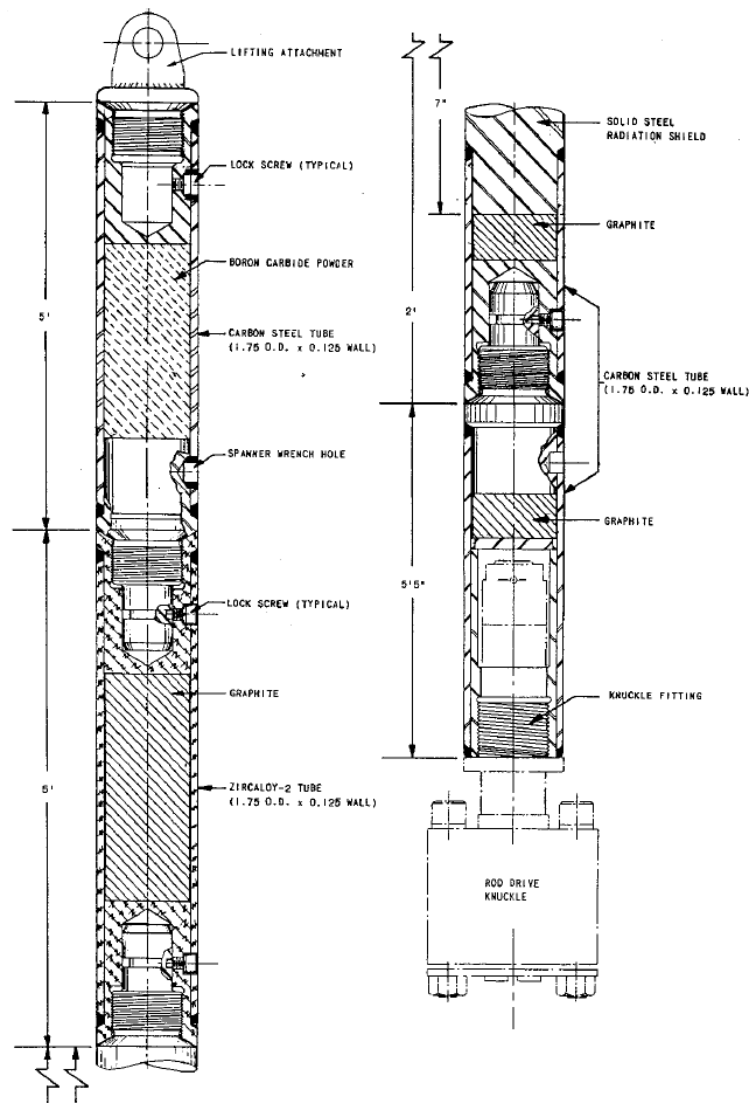


Figure 4. Illustration of the Key Segments of a TREAT Control Rod

2.2 Key Core Properties

Current modeling and simulation of TREAT is challenging due to a number of issues, including long-standing uncertainties in core properties, gaps in TREAT knowledge created by the multi-decade standby in reactor operations, and limitations in the currently-available historic measured data.

One of the most significant uncertainties is the boron impurity of the TREAT fuel. During the fuel manufacturing process, boron migrated from the borated steel separators used in the baking of the fuel, resulting in a boron impurity which is significantly greater than that of typical reactor-grade graphite. Only a limited number of sample measurements have been made to

investigate the fuel boron impurity. The distribution of the boron has not been characterized, and is typically treated as uniform in TREAT modeling (although in reality it is assumed that the impurity may be in higher concentrations near the fuel periphery). From sample measurements, an estimate of 7.6 ± 1.4 ppm boron was evaluated by Iskenerian in 1960 [5]. This value was traditionally accepted as the reference value in TREAT modeling. Recently the data from the historic measurements was re-evaluated at INL as part of an effort to develop a TREAT benchmark, which yielded a calculated mean average content of 5.90 ± 0.35 ppm [6]. The current analysis has used the traditional value of 7.6 ppm.

An additional source of uncertainty is the graphite structure within the TREAT fuel. When the TREAT fuel was manufactured, the fuel-graphite mixture was not brought to the high temperatures necessary to graphitize the carbon (due to concerns regarding the volatilization of the urania). Consequently, the TREAT fuel structure is a complex mixture of both graphitized and un-graphitized carbon. Based on information from the fuel manufacturer, a graphitized-to-total carbon ratio of 0.59 was estimated by TREAT analysts in 1988 [7]. Their analysis found that treating the fuel as partially, rather than fully, graphitized has an effect on both the core eigenvalue and the fission rate of a given test sample within the core. A similar trend was observed more recently at ANL during analyses to support the study of conversion of TREAT to an LEU core [8, 9]. The PROTEUS-SN simulations performed in this study were all done assuming full graphitization, since the focus was on preliminary code-to-code comparisons, with the understanding that the partial graphitization must be accounted for in any future validation work.

3. TREAT Modeling and Simulation

The primary focus of this study was to perform initial simulations of TREAT with the neutron transport code PROTEUS-SN. Supporting work has also been performed using other reactor physics codes. The initial PROTEUS-SN analyses were performed using a cross-section ISOTXS file generated during a historic set of simulations of TREAT done at ANL, which were performed to investigate the feasibility of TREAT analysis with the DIF3D-NODAL code [10]. This cross-section set was generated during the aforementioned historic study using the WIMS-ANL code, with the nine energy group structure documented in Table 1. During the timeframe of the analysis presented in this report, work was also performed at ANL to pursue the use of the Monte Carlo reactor physics code Serpent [11] for cross-section generation [12]. Initial analyses have also been performed with a new Serpent-generated cross-section set.

Table 1. Nine Energy Group Structure in WIMS-ANL-generated ISOTXS file

Group	Upper Bound (eV)
1	1.0000E+7
2	5.0000E+5
3	9.1180E+3
4	1.4873E+2
5	4.0000E+0
6	1.3000E+0
7	6.2500E-1
8	1.8000E-1
9	8.0000E-2

3.1 MCNP Simulations

The Monte Carlo code MCNP [13] was used to evaluate select aspects of TREAT modeling, including the impact of homogenization, the effect of the partial graphitization of the TREAT fuel, and the impact of different ENDF cross-section libraries.

3.1.1 Homogenized Fuel Assembly in Infinite Lattice

To begin investigating the impact of homogenization, MCNP simulations were performed for an infinite lattice of TREAT fuel assemblies, assuming a simplified version of the TREAT assembly geometry. Reflective boundary conditions were applied to the radial surfaces of the assembly, with void boundary conditions above and below the axial reflector region. In the

heterogeneous model, the fuel, gap, cladding, and surrounding air were modeled discretely, including the assembly's chamfered corners. As a simplification, the axial reflector regions were assumed to have the same radial geometry as the fuel region, and the small axial spacers (between the fuel and reflector regions) were ignored, as shown in Figure 5. This model was then homogenized radially to examine the effect. Results are summarized in Table 2. The homogenization of the reflector region causes an under-prediction of the axial neutron leakage, increasing reactivity. The homogenization of the fuel region causes a much smaller change in k -eff, but it is suspected that there may be some cancellation of effects, as discussed in Section □.

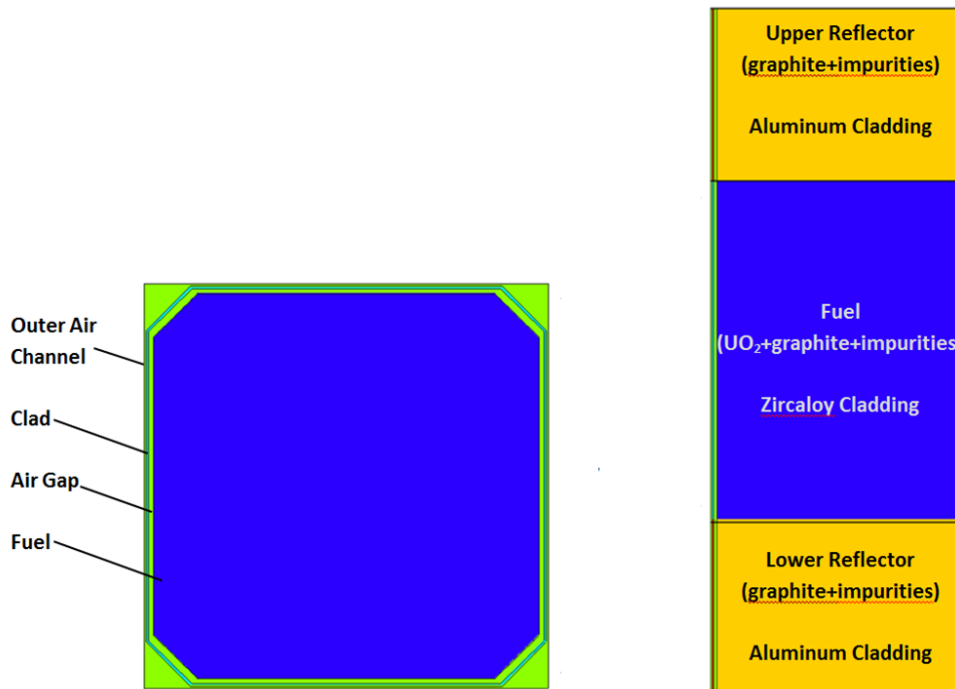


Figure 5. Lengthwise View of TREAT Fuel Assembly in MCNP, (a) Simplified Geometry and (b) True Geometry

Table 2. MCNP Results for Infinite Lattice of Simplified TREAT Fuel Assemblies

Model	k	Δk , pcm
Heterogeneous Fuel Region Heterogeneous Reflector Region	1.45561	
Homogenized Fuel Region Heterogeneous Reflector Region	1.45624	63
Homogenized Fuel Region Homogenized Reflector Region	1.46150	589

* MCNP standard deviation $\sigma \leq 0.00011$

Table 4. MCNP Homogenization Results for More Detailed TREAT Fuel Assembly Model

Homogenized Zone	k-eff	Δk , pcm
None (i.e., heterogeneous case)	1.42617	
5 (fuel region only)	1.42784	167
1, 2, 3 (upper reflector regions only)	1.43109	492
1, 2, 3, 5, 7, 8 (upper & lower reflector, & fuel region)	1.43451	834

* MCNP standard deviation $\sigma \leq 0.00004$

3.1.2 Fuel Graphitization

The impact of accounting for the partial graphitization of the TREAT fuel carbon was evaluated order to obtain a quantitative estimate of its effect. This analysis was done for a core loading similar to that of the TREAT Minimum Critical Core experiment [14], using an MCNP model developed during the historic DIF3D-NODAL analyses [10].

The Minimum Critical Core experiments are a set of experiments done in TREAT during the first six months of operation. They were performed in order to obtain information on reactor characteristics and behavior. This experiment set provides a set of useful data for model validation, including an approach to criticality (incremental addition of assemblies), critical loading, isothermal temperature coefficient of reactivity, neutron flux distribution, and others.

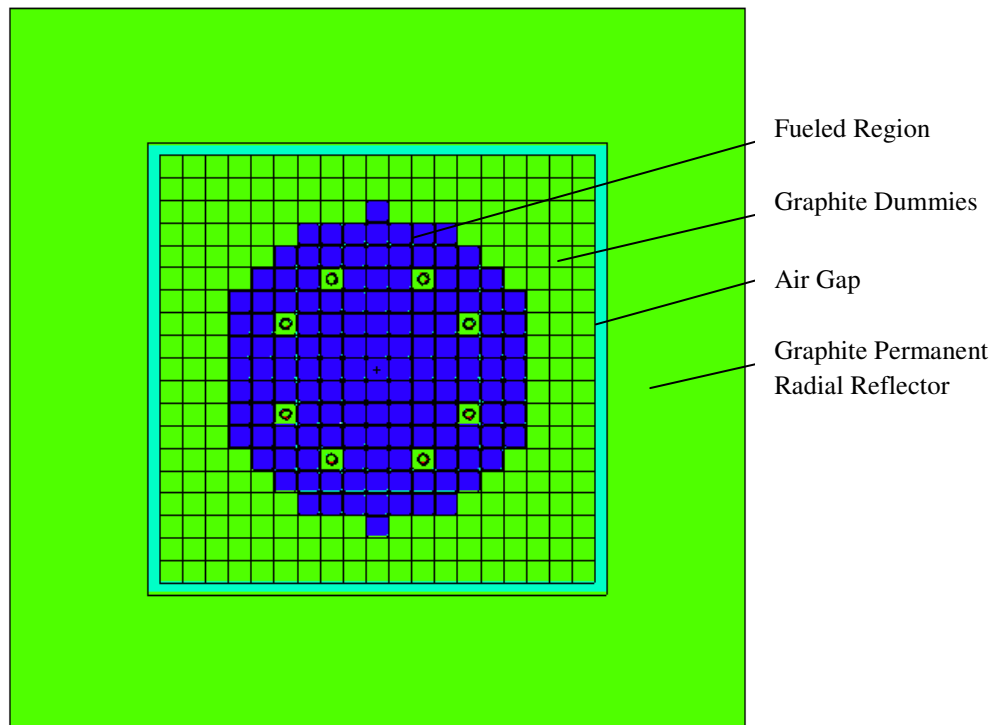


Figure 7. Cross-sectional View of MCNP Model Similar to TREAT Minimum Critical Core

The core loadings used in these experiments provide less complex cases for analysis than the later irradiation experiments, since there are no experiment vehicles and the control rods were fully withdrawn in many of the cases. The current analysis focused on comparing the calculated eigenvalue for a reported critical loading. This experiment featured a small core loading, surrounded by graphite dummy elements, as illustrated in Figure 7. It was performed in the pre-upgrade core. In the model used in this graphitization study, the assemblies surrounding the control rods were modeled as graphite-filled.

The partial graphitization was simulated by applying free-gas and $S(\alpha,\beta)$ treatments to fractions of the fuel carbon, rather than $S(\alpha,\beta)$ to all fuel carbon. Using ENDF/B-VII.0 cross-sections, there was an increase in reactivity, $(k-1)/k$, of 1060 pcm ($\sigma = 7$ pcm) when treating the fuel as partially, rather than fully, graphitized.

3.1.3 Cross-section Library

Analyses were also performed to examine the impact of different ENDF cross-section data libraries. The key focus was on quantifying the effect of the change in carbon absorption cross-section between ENDF/B-VII.0 and ENDF/B-VII.1. Example results are presented in Table 5, again using the same historic Minimum Critical Core model. The increase in carbon absorption cross-section causes a decrease in the calculated eigenvalue of the reactor. When both the fuel and reflector carbon are updated from ENDF/B-VII.0 to VII.1, there is over a decrease of over 1100 pcm in reactivity. A similar trend has been observed in the simulation of other reactors containing significant amounts of carbon [15].

Table 5. TREAT MCNP Modeling with Different Cross-section Libraries

Change in Data (from Reference Model using ENDF/B-VI.0)	Resultant Change in Reactivity, $(k-1)/k$, pcm
ENDF/B-VII.0, all isotopes	147
ENDF/B-VII.1, fuel carbon only	-502
ENDF/B-VII.1, fuel and reflector carbon	-1001

* MCNP standard deviation $\sigma \leq 7$ pcm

3.2 PROTEUS-SN Simulations with Historic ISOTXS File

3.2.1 Homogenized Single Assembly Model

A radially homogenized, simplified-geometry single fuel assembly was simulated in PROTEUS-SN using the historic WIMS-ANL cross-sections. For comparison with MCNP, the homogenized MCNP single assembly model discussed previously was used. For consistency with the cross-section set used in the PROTEUS-SN simulations, the MCNP input was adjusted to ENDF/B-VI.0 cross-sections for the code-to-code comparison. In addition, isotopes in the MCNP input without data available in the PROTEUS-SN cross-section set were removed from

the model, so that the PROTEUS-SN and MCNP simulations assumed identical compositions. Once again, reflective boundary conditions were assumed for the sides of the assembly, with void boundary conditions above and below the reflector region. Two meshes were used in the PROTEUS-SN simulations: 10x10 radial segmentation and 20x20 radial segmentation. Both meshes had 15 axial segments in the fuel region, and 7 in each reflector (Figure 8). The single assembly meshes for PROTEUS were generated using CUBIT [16]. Example results are presented in Table 6.

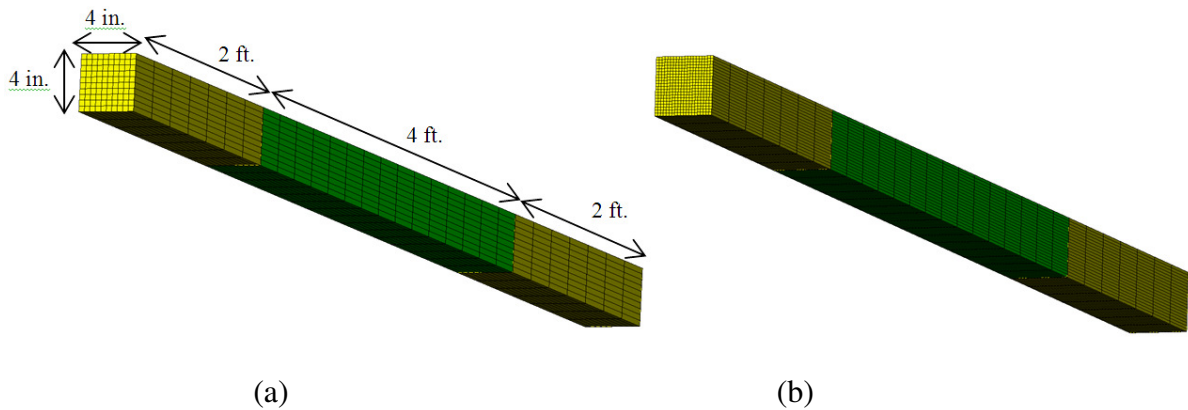


Figure 8. PROTEUS-SN Meshes Used for Infinite Lattice of Homogenized Assemblies, (a) 10x10x29 and (b) 20x20x29

Table 6. Example Results for MCNP and PROTEUS-SN Simulations of Infinite Lattice of Homogenized, Simplified TREAT Fuel Assemblies

Model		k-eff	Δk , pcm
MCNP		1.47915 (0.00011)	
PROTEUS-SN	L1T1, 10x10x29 mesh, P1	1.478776	-37
	L5T5, 10x10x29 mesh, P1	1.479140	-1
	L5T5, 20x20x29 mesh, P1	1.479139	-1
	L5T5, 20x20x29 mesh, P0	1.477034	-212
	L11T11, 20x20x29 mesh, P0	1.477048	-210

* P0: transport cross section used

3.2.2 Full Core Model

Homogenized-assembly full core simulations were performed with PROTEUS-SN for comparison against DIF3D simulations of the historic TREAT Minimum Critical Core model developed in previous studies done at ANL. For this analysis, a set of ANL-developed tools were utilized to convert the DIF3D model to a set of PROTEUS-compatible files. The CCCC_to_PROTEUS.x script and nodal.x code were used for the conversion, and the MT_Makepnt.x script was used to convert the resultant mesh to a .vtk mesh for viewing in

visualization toolkit VisIt [17] to confirm correct conversion. In the historic DIF3D model, the full radial reflector was not included and an albedo boundary condition was employed. In the PROTEUS-SN simulations, a void boundary condition was used, and for comparison the DIF3D model was rerun with a void boundary condition as well. The focus of this analysis was code-to-code comparison, and therefore the reduced dimension of the radial reflector was neglected.

The historic DIF3D simulations were performed with DIF3D-nodal, but the use of VARIANT nodal transport was also explored. The historic simulations found that VARIANT with P0 scattering cross-sections gave similar results to DIF3D-nodal, while VARIANT P1 differed. The updated simulations with a void boundary condition showed similar behavior, as documented in Table 7. According to the memo on the previous studies, these trends were thought to be due to the nature of the historic cross-section generation [10]. This was not investigated further at this time, since the recent studies with the historic cross-section set were meant to serve as initial analyses, with updated simulations with the new cross-section sets to follow.

Table 7. DIF3D Results for Historic Minimum Critical Core Model with Void Boundary Conditions

Solution Option		k_{eff}	$(k-1)/k$, pcm
DIF3D-nodal		1.005454	542
VARIANT	P1	1.012114	1197
	P0	1.006964	692

* P0: transport cross section used

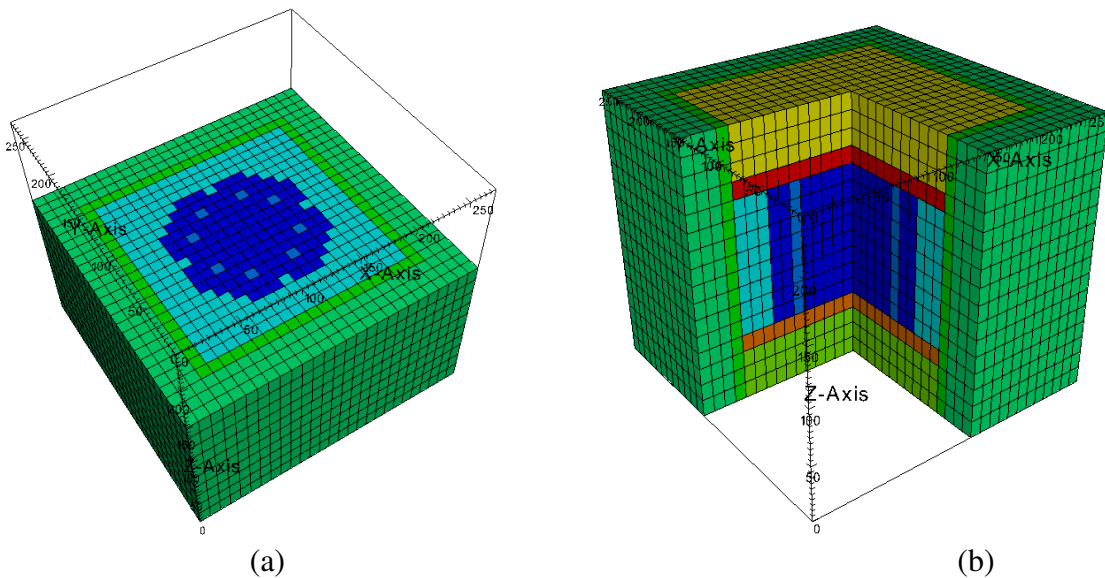


Figure 9. PROTEUS-SN Model for TREAT, (a) Radial Slice and (b) Axial Slice

To compare against MCNP as well, a new MCNP input was constructed which exactly models the geometry (including the reduced radial reflector) and compositions assumed in the DIF3D and PROTEUS-SN simulations. Again ENDF/B-VI.0 cross-section libraries were used, to eliminate the impact of differences in cross-section data. In addition, the MCNP model used only isotopes present in the PROTEUS-SN model. The original DIF3D model featured a reduced radial reflector with an albedo boundary condition. For the current code-to-code comparisons, this geometry was still used, now assuming a void boundary condition. The PROTEUS-SN model (which is the same as the DIF3D model) is shown in Figure 9, and the MCNP model in Figure 10.

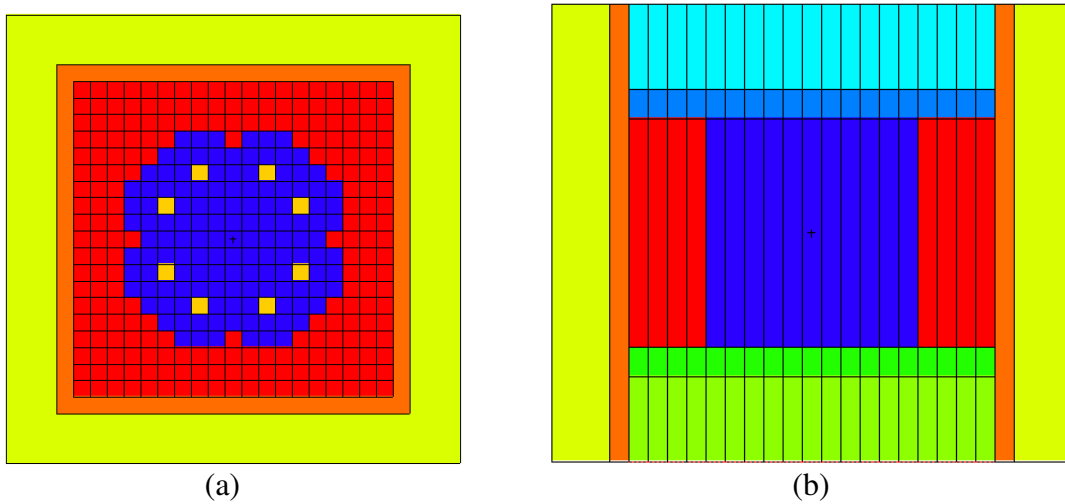


Figure 10. MCNP TREAT Core, (a) X-Y View and (b) X-Z View

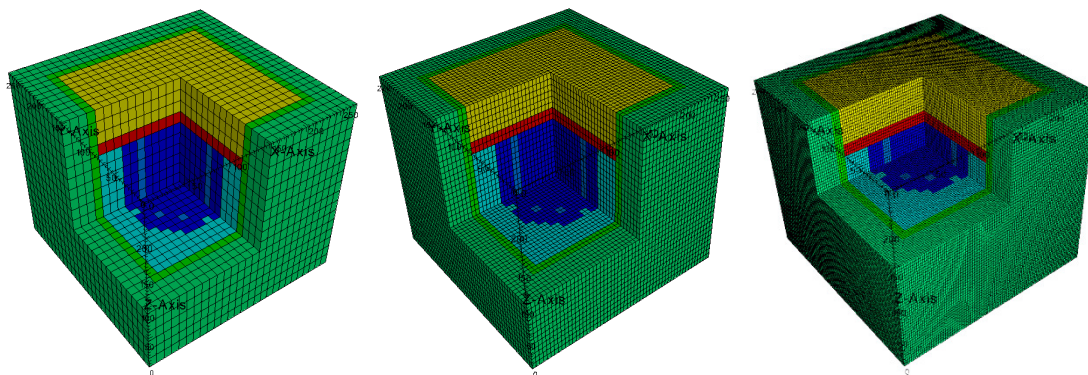


Figure 11. Meshes Used in Current PROTEUS-SN Simulations – A, B, and C

PROTEUS-SN simulations were performed for three different meshing schemes. The first used the original DIF3D mesh, which features 10.16" (i.e. the width of a single fuel assembly) cells in the x- and y-directions, with 16 axial segments. The additional simulations were performed doubling, and then quadrupling the refinement of the original mesh (as shown in Figure 11). Results are summarized in Table 8.

Table 8. PROTEUS, MCNP, and DIF3D Results for Minimum Critical TREAT Core with Homogenized Assemblies and Reduced Radial Permanent Reflector

MCNP				k_{eff}
				1.00872 (0.00019)
PROTEUS	Solution Option			k_{eff}
	Scatter Order	Mesh	Angle	
	P1	A	L1T1	1.009725
			L3T2	1.009721
		B	L3T2	1.011335
			L5T5	1.011329
			L7T8	1.011333
		C	L3T2	1.011726
	L11T11		1.011724	
	P0	A	L3T2	1.004608
		B	L3T2	1.006222
		C	L3T2	1.006615
			L11T11	1.006614
DIF3D	Solution Option			k_{eff}
	VARIANT	P1		1.012114
		P0		1.006964
	Nodal			1.005454

* P0: transport cross section used

3.3 Serpent Model Simulations

In support of the TREAT analysis with PROTEUS-SN, modeling of TREAT with the Monte Carlo code Serpent was performed. The objective of this work was to eventually use Serpent to generate multi-group cross-sections to be converted into a PROTEUS-compatible ISOTXS file, using the recently developed ANL tool [12].

As an initial step, a single standard fuel assembly was evaluated. This was performed again using a simplified model which ignores detailed design features (indentations, outgas tubes, spacers, etc.), as illustrated in Figure 12 (the same geometry as assumed in the MCNP analyses). The fuel and reflector regions were both assumed to have a 25 mil cladding thickness, with a 50 mil gap on the fuel sides. The fuel assembly was simulated in both an infinite lattice (reflective boundary conditions on x- and y-faces and void boundary conditions above/below axial reflectors), and in a finite 19x19 lattice. Simulation results were compared against results generated by MCNP5, with ENDF/B-VII.0 cross-section data used for both codes. The models were evaluated under both cold core and heated (600K) conditions. Results are summarized in Table 9.

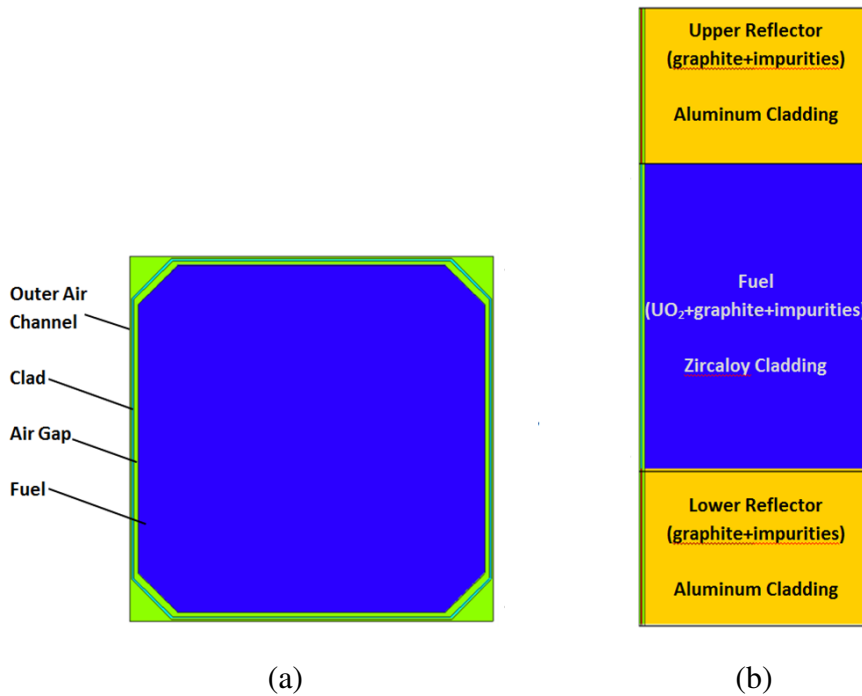


Figure 12. Simplified Model of TREAT Fuel Assembly Used in MCNP and Serpent, (a) X-Y and (b) X-Z View

The reasons for the discrepancies between the codes are still being investigated, but are assumed to be due to minor differences in the cross-section data. However, this does not have an impact on the focus of this study, because for consistency the subsequent PROTEUS-SN simulations with Serpent-generated cross-sections were evaluated for code-to-code comparison with the Serpent simulation results. From the above data, temperature reactivity feedback coefficient values were also estimated (Table 10). There is significantly more negative feedback with heat-up in the finite lattice. This is because temperature reactivity feedback in TREAT primarily comes from increased leakage (as neutrons come into thermal equilibrium with the fuel graphite). The fuel is highly enriched (~93%), so there is comparatively very little Doppler feedback.

Table 9. MCNP and Serpent Simulation Results for Simplified TREAT Fuel Assembly

	Model	Code	k-eff
Cold*	Infinite Lattice	Serpent	1.45312
		MCNP	1.45594
	19x19 Lattice	Serpent	1.09149
		MCNP	1.09528
600K	Infinite Lattice	Serpent	1.43027
		MCNP	1.43265
	19x19 Lattice	Serpent	1.04743
		MCNP	1.04977

* 293.6K for MCNP, 300K for Serpent

Table 10. Temperature Reactivity Feedback Estimate for MCNP and Serpent Simulations of Infinite and 19x19 Fuel Assembly Arrays

	$\Delta(k-1)/k$, pcm, per $\Delta^\circ\text{K}$, cold* \rightarrow 600	
	MCNP	Serpent
Infinite Lattice	-3.64	-3.66
19x19 Lattice	-12.92	-12.85

* 293.6K for MCNP; 300K for Serpent

In order to further evaluate the impact of homogenization in TREAT simulations, a series of homogenization studies were also performed with the single assembly Serpent model. First, homogenization was evaluated for a 2D model of the fuel region only, for an infinite lattice, using the region volume fractions documented in Table 11 to generate the homogenized composition. Results are presented in Table 12. Homogenization of the 3D simplified model of the fuel assembly was also evaluated, as presented in

Table 13. As discussed above, in the simplified model the reflector block, gap, and cladding were assumed to have the same dimensions as the fuel regions, and therefore the volume fractions in Table 11 were also used in the homogenization of the reflector regions.

In the 3D case, the homogenization of the reflector and fuel regions caused an increase in k-eff, due to the decrease in axial neutron leakage. The homogenization of the fuel region only in the 3D model showed a significantly smaller increase in k-eff, while the 2D homogenization of

the fuel region indicated that the homogenization causes a decrease in k relative to the heterogeneous model. This behavior is still being investigated further, but it is assumed that there may be some cancellation of effects occurring in the 3D model of the fuel region (as the smearing together of the fuel with the gap and clad tends to decrease k (observed in the 2D case), but the decrease in leakage when a finite axial dimension is considered tends to increase k -eff). The 3D Serpent results shown in

Table 13 are consistent with the trends observed in the MCNP simulations discussed previously (Table 2).

Table 11. Volume Fractions Used in Homogenization of TREAT Assembly

Region	Volume Fraction
Fuel	0.883852
Cladding	0.023002
Air Outside	0.044313
Fuel-to-clad Air Gap	0.048834

Table 12. 2D Serpent Simulation of TREAT Assembly Fuel Region

	k -inf	Δk , pcm
Heterogeneous	1.68269 (0.00005)	
Homogeneous	1.67901 (0.00009)	-368

Table 13. 3D Serpent Simulation of Simplified TREAT Fuel Assembly

Model	k -eff	Δk , pcm
Heterogeneous Fuel Region Heterogeneous Reflector Region	1.45312	
Homogenized Fuel Region Heterogeneous Reflector Region	1.45906	94
Homogenized Fuel Region Homogenized Reflector Region	1.45406	594

* Serpent standard deviation $\sigma \leq 0.00022$

3.4 Multigroup Cross Section Generation

Multigroup cross sections can be generated using deterministic or Monte Carlo tools. Since the geometry of the TREAT assembly is different from regular pin cells with cylindrical, Cartesian, or hexagonal geometry, it normally needs a geometric approximation when using a

deterministic tool. Preliminary Monte Carlo calculations were performed for a single fuel assembly with a heterogeneous geometry, a homogeneous composition, or a pin cell geometry with equivalent volumes to the original geometry. The k-inf solutions from a single fuel assembly with heterogeneous or homogeneous geometries are a little different from Table 14 because of slightly different compositions and volume fractions and the use of MCNP instead of Serpent. Nevertheless, the magnitude of the heterogeneity effect is similar to Table 14.

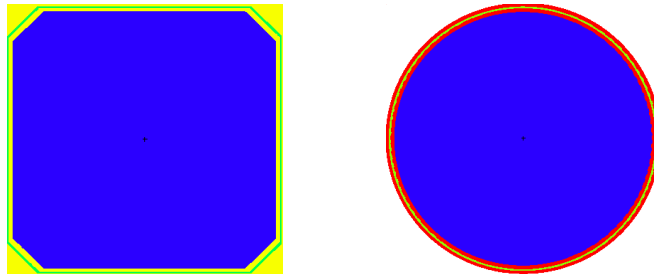


Figure 13. Geometries for Generating TREAT Fuel Assembly Cross Sections

Table 14. MCNP Eigenvalues of TREAT Fuel Assembly with Different Geometries

Geometry	k-inf	Δk , pcm
Exact heterogeneous	1.68368 \pm 0.00014	
Equivalent cylindrical pin	1.68344 \pm 0.00013	-24
Homogeneous	1.67876 \pm 0.00012	-492

The conversion to a cylindrical geometry appears to be reasonable because the eigenvalue difference between the exact heterogeneous and cylindrical geometries is only 24 pcm. However, the generation of cross sections for reflector and control rod assemblies requires supercell-type calculations which introduce additional approximations and errors. In addition, due to a large neutron streaming effect to the axial direction through air channels, heterogeneous cross sections should be generated for accurate solutions. Since PROTEUS requires testing transport solutions with accurate heterogeneous cross sections before using the cross section API which generates heterogeneous cross sections on the fly, assembly-homogeneous or heterogeneous cross sections were generated using Serpent.

Serpent includes a capability of generating multigroup (MG) cross sections which would be useful to perform core analysis as well as to benchmark cross sections generated by deterministic approaches. The MG cross sections generated from Serpent have the following limitations:

- Macroscopic cross sections only: i.e., no isotopic microscopic cross sections,
- P_N total scattering matrices only: i.e., no partial scattering matrices such as elastic, inelastic, $n2n$, and $n3n$ cross sections,
- No high-order P_N total cross sections,
- No partial principle cross sections such as (n,α) , (n,p) , (n,d) , and (n,t) which are included in the capture cross section.

Due to the limitations above, the MG cross sections generated from Serpent are so far adequate to use for diffusion calculation codes. In addition, many-group cross sections (more than a few tens groups) as well as higher-order P_N scattering matrices requires thorough verification tests.

To use the MG cross sections generated from Serpent in PROTEUS, a computer code was developed which reads the Serpent cross section output (the .m file) and produce a cross section file in the ISOTXS format.

Since the contribution of the (n,2n) cross sections is significant for fast reactor analysis, those cross sections need to be separate from the total scattering cross section matrices. In addition, the high-order P_N total cross sections are needed for accurate transport calculations.

To provide the data missing in the Serpent for accurate reactor analysis, the MC²-3 cross sections were utilized when converting the Serpent cross section output to the ISOTXS format. Under the assumption that scattering matrices do not change much, those for P_N total and (n,2n) are obtained from MC²-3, as shown in Figure 14. One may use the GROUPT module of NJOY instead of MC²-3. For thermal reactor applications, however, the contributions of (n,2n) cross sections would be very small.

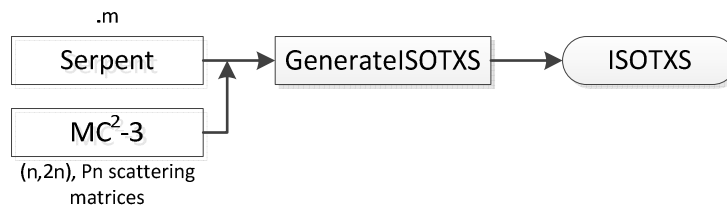


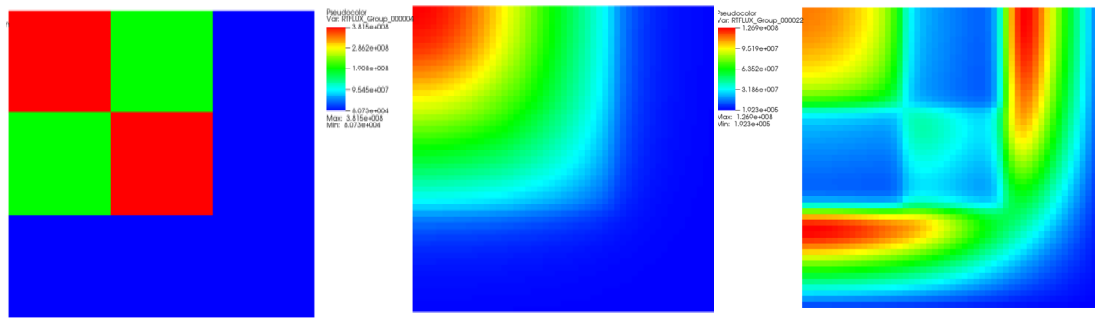
Figure 14. ISOTXS Generation Using Serpent Multigroup Cross Section

Preliminary verification tests were conducted using the C5 benchmark problem, indicating that the Serpent eigenvalues for pin cells and fuel assemblies were well reproduced with the ISOTXS files generated from Serpent. For a 2D core calculation, the 23-group cross sections for the UO₂ and MOX fuel assemblies were provided using Serpent, and those for the water reflector were generated using the two-region problem with water and UO₂ assemblies from which the cross sections for the water region only were tallied.

As shown in Table 15, the eigenvalue difference between MCNP and diffusion for the 2D C5 benchmark problem (shown in Figure 15) is only -34 pcm which is smaller than the differences (up to 137 pcm Δk) between MCNP and Serpent observed for fuel assemblies. The smaller eigenvalue difference in the core calculation may happen due to error cancellations. The eigenvalue difference between MCNP and Serpent would be greatly reduced when the same cross section library was used for both codes. This test result indicates that the MG cross sections in the ISOTXS form generated using Serpent works well for thermal problems.

Due to the complex geometry of TREAT, multigroup cross sections (9 groups and 23 groups) were generated using Serpent. Those cross sections were saved in the ISOTXS format using the conversion tool discussed above. For more accurate solutions accounting for actual problem neutron spectra, the MG assembly-homogeneous or heterogeneous cross sections were generated using the 3D fuel assembly problem or the 3D fuel core problem which is to be solved. For

example, neutron spectra are different depending upon problems which have relatively larger or smaller amount of graphite, as shown in Figure 16.



(Composition Assignment) (Fast Spectrum: 300 keV) (Thermal Spectrum: 0.1 eV)

Figure 15. Composition Assignment and Fast and Thermal Fluxes of the C5 Problem Resulting from Diffusion Calculation with the 23-group Multigroup Cross Sections from Serpent

Table 15. Eigenvalue Comparison for the C5 Benchmark Problem between MCNP, Serpent, and Diffusion (23-group MG cross sections)

Case	MCNP	Serpent (pcm Δk)	Diffusion (pcm Δk)
MOX FA (7.4 w/o)	1.21171	-137	
UOX FA (3.1 w/o)	1.39025	-99	
2D Core	1.19448		-34

* Standard deviation of MCNP and Serpent ≤ 20 pcm

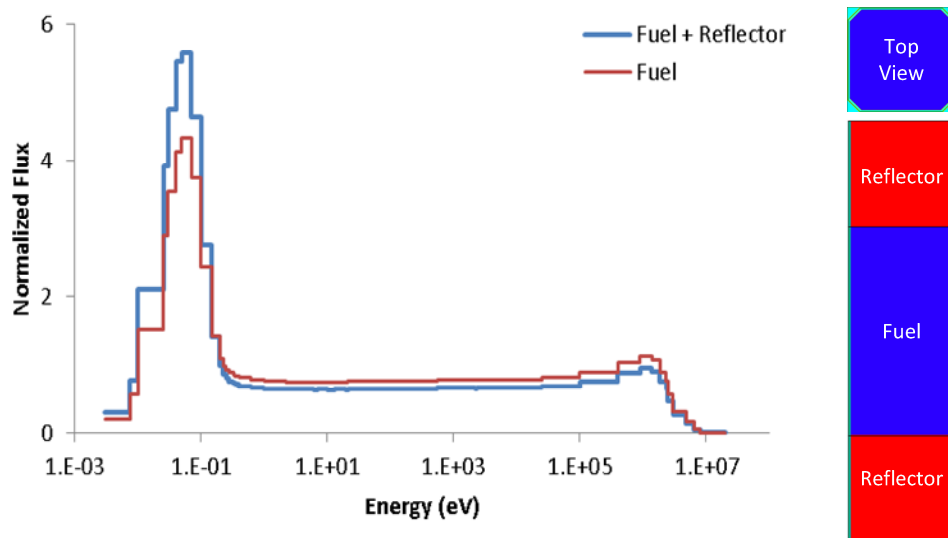


Figure 16. 3D Fuel Assembly Problem (right) and Its Neutron Spectra (left) for TREAT

For verification tests of MG cross sections, 3D full core problems based on the minimum critical core were solved using the MG cross sections generated from Serpent. Since it has been observed that the neutron streaming effect in the axial direction is significant, the 3D full core problems with homogenized assembly configurations were solved using Serpent and diffusion codes to compare eigenvalue solutions. Note that no air channel was modelled in these verification calculations.

As shown in Table 19, eigenvalue agreed well between Serpent and Diffusion calculations for cases with or without graphite assemblies at the eight control rod locations. This indicates that the MG cross sections generated from Serpent works well for TREAT problems. However, these solutions are more than several hundreds of pcm off from the Monte Carlo solution with the heterogeneous geometry. Therefore, the assembly-homogeneous cross sections require direction-dependent discontinuity factors and/or diffusion coefficients to accurately estimate currents between assemblies (fuel, control rod, reflector, and air gap). Further tests and analyses for heterogeneous MGs cross sections will be discussed in the following sections.

Table 16. Eigenvalues for 3D Full Core Problems (No Air Regions) with Different FA and CR Assembly Loadings

Case	Serpent	Diffusion	Δk (pcm)
All Fuel Assemblies	1.15926	1.16079	153
8 Graphite Assemblies	1.14746	1.14902	156

3.5 PROTEUS-SN Simulations with Serpent-generated Cross-sections

Initial PROTEUS-SN simulations were performed with the new Serpent-generated cross-section sets. The meshes for this analysis were created by first using CUBIT to generate exodus meshes, which were then converted to PROTEUS-compatible .ascii meshes with the ANL-developed ExodusConverter.x conversion tool. The Serpent-generated cross-sections included heterogeneous and homogeneous 9 and 23 group sets.

Initial comparisons were made using a 2D heterogeneous model of the fuel region, with the 9 group cross-section set. Results are presented in Table 17 for two different example meshes (illustrated in Figure 17). Even with the coarser of the two meshes, the eigenvalue agrees well with Serpent. However, future mesh refinement studies must of course also evaluate how well the solution agrees in other, more detailed parameters. For example, the thermal flux distributions for the three cases presented in Table 17 differ, as illustrated in Figure 18. Parameters such as this will be evaluated in greater detail in the mesh refinement studies included in future validation and verification work. The 2D model was also evaluated for a PROTEUS-SN simulation using a homogenized fuel region and the homogeneous Serpent-generated cross-sections, to begin evaluating whether the homogeneous cross-sections capture the behavior. Example results are shown in Table 19.

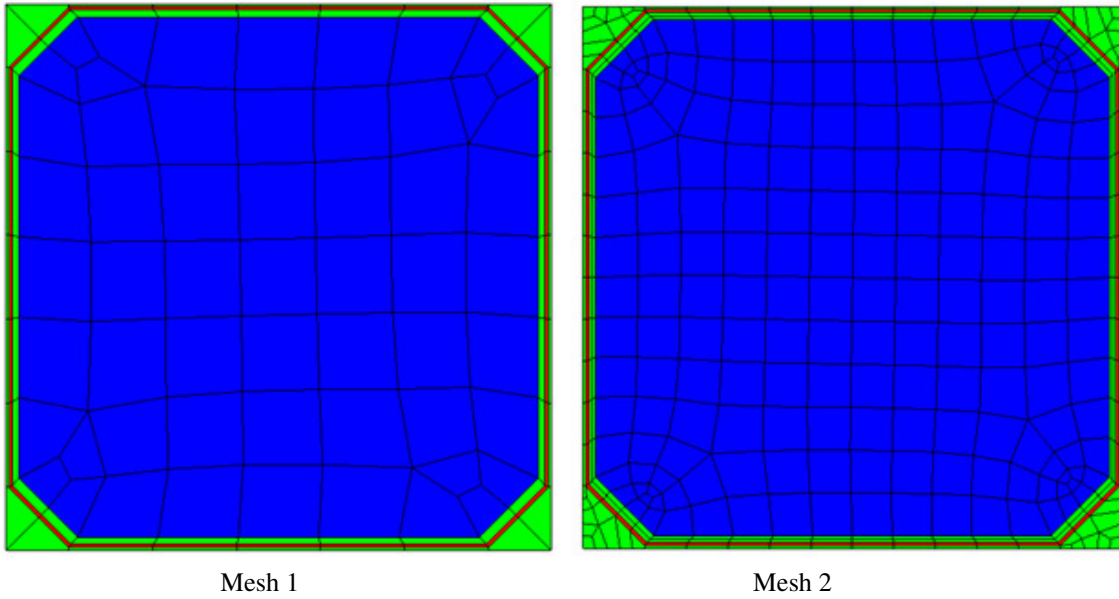


Figure 17. Example PROTEUS-SN Meshes for TREAT 2D Fuel Assembly Heterogeneous Fuel Region

Table 17. PROTEUS-SN Results, 2D TREAT Assembly Heterogeneous Fuel Region

Code		k-inf
Serpent		1.68269 (0.00005)
PROTEUS	Case 1: mesh 1, L1T1, P1	1.682775
	Case 2: mesh 1, L5T5, P1	1.682805
	Case 3: mesh 2, L5T5, P1	1.682817

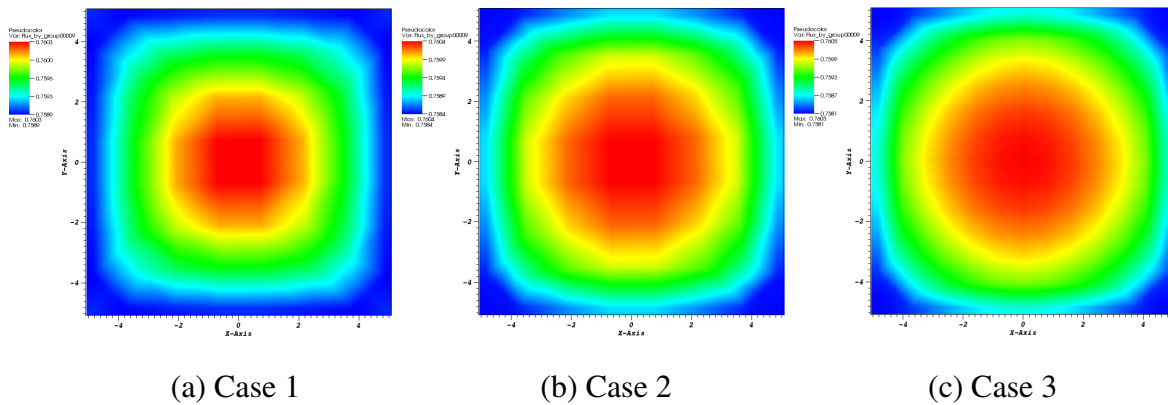


Figure 18 Thermal Neutron Fluxes for PROTEUS-SN 2D Heterogeneous Fuel Region

Table 18. 2D TREAT Fuel Region, Evaluation of PROTEUS-SN Simulation with Serpent-generated Homogenized Cross-sections

Model	k-inf
Serpent Heterogeneous	1.68269 (0.00005)
PROTEUS, Heterogeneous Cross-section set	1.682817
PROTEUS, Homogeneous Cross-section Set	1.683530

3D single assembly heterogeneous meshes for PROTEUS-SN were also generated using CUBIT and the mesh conversion tool. Examples are shown in Figure 19. Analysis of the 3D heterogeneous model is in progress, and there are not finalized results to present at this time.

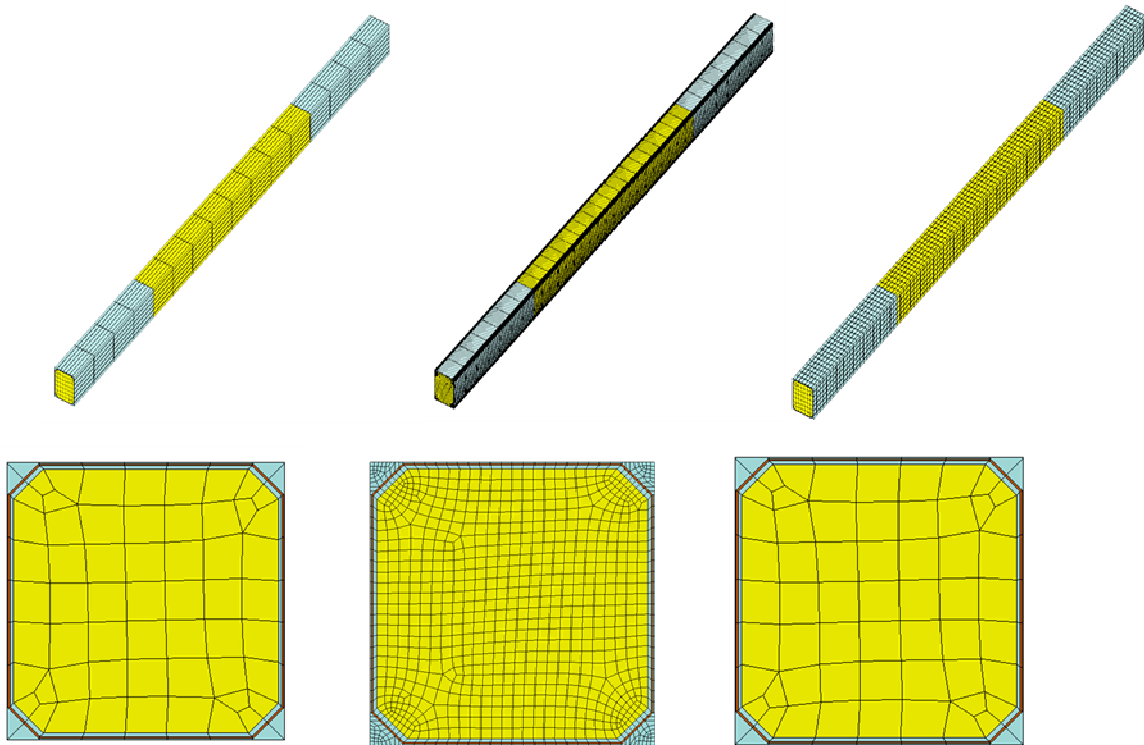


Figure 19. Example 3D Heterogeneous TREAT Fuel Assembly Meshes for PROTEUS-SN

Simulation of the 3D heterogeneous model has proven challenging due to the air gaps between the fuel and cladding and the air sections outside the cladding between adjacent fuel assemblies. These air regions made it very challenging for the simulation to run to a converged solution, even when utilizing large computing clusters. Therefore, for these preliminary investigations, simulations were performed using a hypothetical higher density material in the gap in order to proceed with code-to-code comparisons. Example results are shown in Table 19, for a PROTEUS-SN with the convergence tolerances set very loose to allow the simulation to

complete. Per discussions with the code developers, the composition of the air regions will be adjusted in future analyses for improved simulation.

Table 19. Results for 3D Heterogeneous TREAT Assembly with Hypothetical Higher Density Material in the Gap

Code	k-eff
Serpent	1.41871 (0.00027)
PROTEUS-SN	1.41717

Initial studies are also currently being performed for 3D multi-assembly core models, which include standard, graphite dummy, and control rod assemblies. An example model is shown in Figure 20. This model features the Minimum Critical Core loading, but has the control rod poison section inserted. Only the core region is included in these preliminary analyses, with the surrounding radial reflector and concrete bioshield omitted. An illustration of the assembly layout is provided in Figure 21. A very coarse mesh was used for these initial simulations, as shown in the 2D illustration of the control rod assembly mesh in Figure 22.

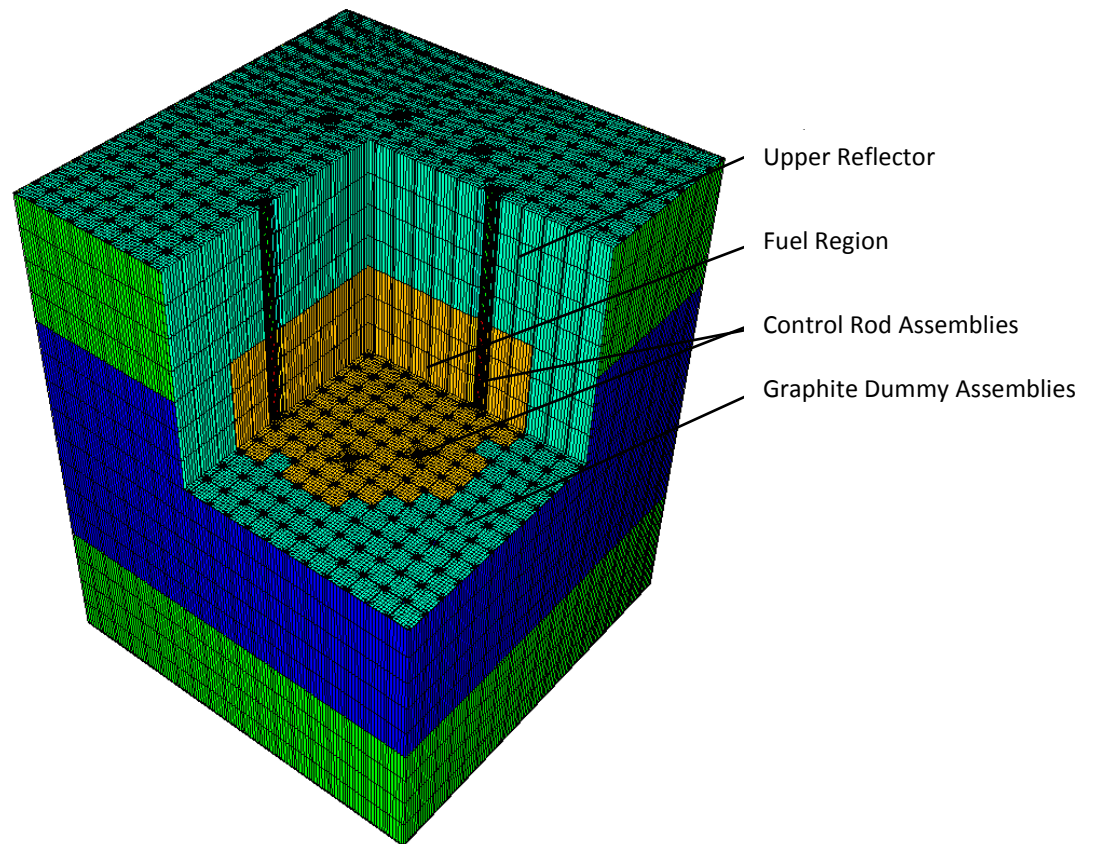


Figure 20. 3D PROTEUS Model of TREAT Minimum Critical Core Loading

For this study, CUBIT was again used to create the individual assembly exodus meshes, which were then converted to PROTEUS-compatible .ascii meshes with the ExodusConverter.x tool. The core mesh was built by merging the individual assembly meshes with the MT_RadialLattice.x tool, which is part of the ANL-developed PROTEUS meshing tool set [18]. Analysis of the heterogeneous full core model is still in progress. There are no code-to-code comparison results to report at this time, and refinement studies still need to be performed. However, general trends can be observed from the initial studies. As an example, the $Nu \cdot Fission$ rate distribution is illustrated in Figure 23, across the fuel axial mid-height.

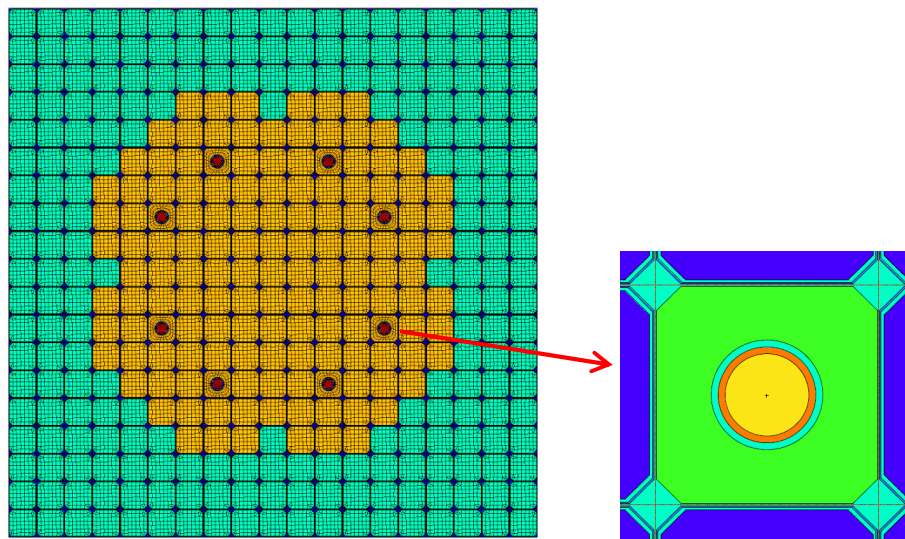


Figure 21. Cross-section View of Example PROTEUS 3D Minimum Critical Core Mesh

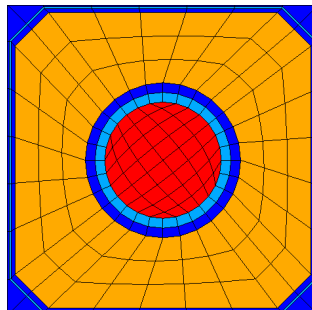


Figure 22. Cross-section View of Coarse PROTEUS Mesh for Control Rod Assembly

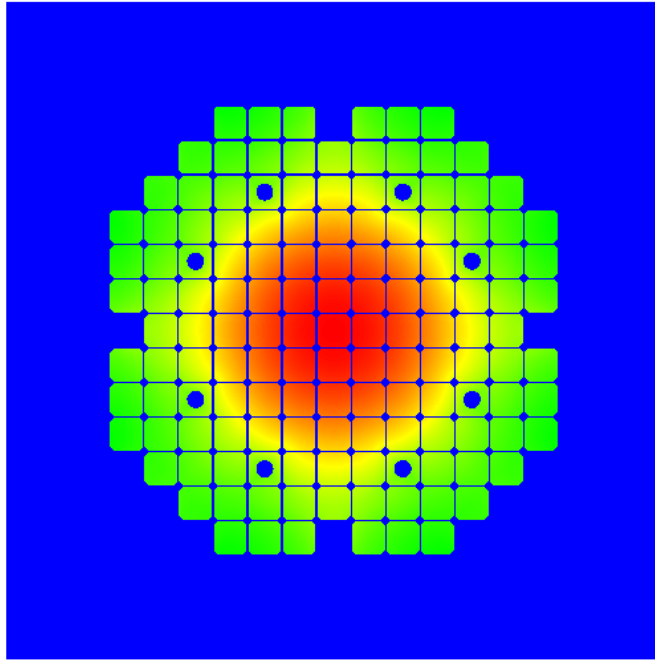


Figure 23. Nu*Fission Rate Distribution at Fuel Section Mid-height in PROTEUS 3D Simulation of TREAT Minimum Critical Core with Control Rod Inserted

4. Conclusions

The PROTEUS neutron transport code has been utilized to perform preliminary simulations of TREAT. Both homogenized and heterogeneous single assembly models and full-core assembly-homogenized models of the historic Minimum Critical Core experiment have been evaluated. To support this work, additional simulations were also performed using the reactor physics codes DIF3D, MCNP, and Serpent. The meshes for the PROTEUS-SN simulations were generated using the CUBIT toolkit, along with ANL-developed mesh merging and conversion tools. The initial PROTEUS-SN simulations were performed using a historic cross-section set generated with the WIMS-ANL code. Simultaneous to this work, efforts were made to develop a method for generating new cross-sections using Serpent. Preliminary simulations with the new cross-section set have also been performed.

The homogenization studies indicated that homogenizing across the air gaps causes an under-prediction of axial neutron leakage, leading to an increase in k -eff. This behavior was observed in both the MCNP and Serpent simulations.

A historic cross-section set was used to evaluate both an infinite lattice of radially homogenized assemblies and a full core model similar to the Minimum Critical Core, featuring radially homogenized standard, control, and dummy assemblies. Simulations were performed using new Serpent-generated cross-section sets. The PROTEUS-SN simulation of the 2D heterogeneous model of the fuel section showed good agreement with Serpent. There were challenges in simulating the 3D heterogeneous model due to the air regions, which will be addressed further in future work.

The analysis of TREAT with PROTEUS-SN is an ongoing task. Key challenges in the modeling have been identified through the current work, and will be addressed moving forward. Additional code-to-code verification and validation with best-available measured data will be performed, and the models and analysis methods will continue to be refined. Future analysis will evaluate actual historic experiments in greater detail, including the Minimum Critical Core experiment series and measured test sample irradiation experiments. Both steady-state and transient operations will be considered.

REFERENCES

1. E. R. Shemon, M. A. Smith, and C. H. Lee, "PROTEUS-SN Methodology Manual," ANL/NE-14/5, Argonne National Laboratory, June 30, 2014.
2. E. R. Shemon, M. A. Smith, C. H. Lee, and A. Marin-Lafleche "PROTEUS-SN User Manual," ANL/NE-14/6, Argonne National Laboratory, June 30, 2014.
3. U. S. Department of Energy, "Resumption of Transient Testing Capability," April 15, 2013, <http://www.energy.gov/ne/articles/resumption-transient-testing>.
4. G. A. Freund, et al., "Design Summary Report on the Transient Reactor Test Facility (TREAT)," ANL-6034, Argonne National Laboratory, 1960.
5. H. P. Iskenderian, "Post Criticality Studies on the TREAT Reactor", ANL-6115, Argonne National Laboratory, 1960.
6. J. D. Bess and M. D. DeHart, "TREAT Fuel Assembly Characterization for Modern Neutronics Validation Methods," Transactions of the American Nuclear Society, Vol. 112, pp. 373-376, San Antonio, Texas, June 7-11, 2015.
7. R. W. Swanson and L. J. Harrison, "The Effect of Carbon Crystal Structure on TREAT Reactor Physics Calculations," 1988 International Reactor Physics Conference, Jackson Hole, Wyoming, September 18-21, 1988.
8. D. C. Kontogeorgakos, H. M. Connaway, A. E. Wright, G. Yesilyurt, K. L. Derstine, M. D. DeHart, and S. R. Morrell, "Neutronics Analyses for an LEU Core for TREAT," Transactions of the American Nuclear Society, Vol. 111, pp. 1248-1251, Anaheim, California, November 9-13, 2014.
9. D. C. Kontogeorgakos, H. M. Connaway, G. Yesilyurt, and A. E. Wright, "Neutronic Analysis of the Minimum Original HEU TREAT Core," ANL/GTRI/TM-14/13, Argonne National Laboratory, April 2014.
10. T. A. Taiwo, Private Communication, Argonne National Laboratory, March 2000.
11. J. Leppanen, "Serpent – a Continuous-energy Monte Carlo Reactor Physics Burnup Calculation Code," VTT Technical Research Centre of Finland, June 18, 2015.
12. C. H. Lee, et al., "FY15 Report on NEAMS Neutronics Activities," ANL/NE-15/23, Argonne National Laboratory, 2015.
13. X-5 Monte Carlo Team, "MCNP – A General N-Particle Transport Code, Version 5 – Volume I: Overview and Theory," LA-UR-03-1987, Los Alamos National Laboratory, 2003.
14. F. Kirn, J. Boland, H. Lawroski, and R. Cook, "Reactor Physics Measurements in TREAT," ANL-6173, Argonne National Laboratory, October 1960.
15. C. J. Diez, et al., "Review of the $^{nat}\text{C}(n,\gamma)$ Cross-Section and Criticality Calculations of the Graphite Moderated Reactor BR1," Annals of Nuclear Energy **60**, 210-217, 2013.
16. CUBIT Web page, www.cubit.sandia.gov.
17. VisIt User's Manual, Version 1.5, UCRL-SM-220449, October 2005.

18. M. A. Smith and E. Shemon, "User Manual for the PROTEUS Mesh Tools, Revision 1.0," ANL/NE-15/17 (Rev. 1.0), Argonne National Laboratory, June 1, 2015.



Nuclear Engineering Division

Argonne National Laboratory
9700 South Cass Avenue, Bldg. 208
Argonne, IL 60439-4842

www.anl.gov



U.S. DEPARTMENT OF
ENERGY

Argonne National Laboratory is a U.S. Department of Energy
laboratory managed by UChicago Argonne, LLC